

LBM SIMULATION OF THE QUASI-STATIC FLOW IN A CLARINET

Yong Shi¹⁾, Andrey R. da Silva²⁾, Gary P. Scavone¹⁾

¹⁾ Computational Acoustic Modeling Laboratory,
Centre for Interdisciplinary Research in Music Media and Technology,
Schulich School of Music, McGill University,
Montreal, Quebec, Canada.
yong.shi2@mail.mcgill.ca, gary.scavone@mcgill.ca

²⁾ Laboratory of Vibrations and Acoustics, Department of Mechanical Engineering,
Federal University of Santa Catarina, Florianopolis - SC - Brazil.
andrey.rs@ufsc.br

ABSTRACT

This paper investigates the nonlinear characteristics of the mouthpiece-reed system of a clarinet using the lattice Boltzmann method (LBM) in a two dimensional domain. The mouthpiece has been investigated for cases of both a fixed reed and a moving reed, with the outlet of the mouthpiece being replaced by an absorbing boundary to thwart possible acoustic oscillations. The influence of the geometry of reed channel has been investigated. Numerical results are compared to the quasi-stationary model based on a simplified memoryless reed and the Bernoulli flow.

1. INTRODUCTION

A clarinet can be roughly divided into a non-linear active component (the mouthpiece-reed system) and a linear passive component (the instrument's resonant bore). The sound production of a clarinet depends on flow-induced vibrations, with the reed modulating the air flow entering into the instrument by opening and closing a narrow channel defined between the reed tip and the lay of the mouthpiece.

Previous studies on the resonator components have produced many useful discoveries and satisfactory models. On the other hand, studies on the non-linear mouthpiece-reed system have been relatively less reported. The characteristic of the mouthpiece-reed system is defined as the non-linear relationship of the volume flow and the pressure difference across the reed channel. Since the pioneering work of Backus [1], the non-linear function of single-reed woodwind instruments has been investigated experimentally and theoretically by a number of authors ([2], [3], [4], [5], [6], [7], [8], [9], [10]).

Besides traditional experimental and theoretical approaches, computational simulations have become popular in the field of musical acoustics thanks to the development of new numerical algorithms and inexpensive computers. Numerical simulations have advantages related to precise parametric control, as well as in certain situations where experimental measurements and theoretical modeling are either very difficult or impossible.

The present paper provides a numerical investigation of the nonlinear element and the physical phenomena involved using a relatively new computational fluid dynamic (CFD) tool called the lattice Boltzmann method (LBM). Compared to other traditional CFD techniques, the main advantage of LBM is rep-

resented by its simplicity in simulating the interactions of the moving reed, the air flow and the acoustic field directly and simultaneously. Also, LBM is well suited for parallel computation, which is advantageous for problems involving complicated geometries and long simulation times.

To obtain the complete characteristics of the reed, the volume flow must be measured in a quasi-static condition, i.e., the air flow is free to pass through the reed channel and the transfer of momentum between the fluid and the reed is neglected. For a fixed reed, it is easy to obtain a quasi-static condition in the simulations. But for the case of a freely moving reed, a tiny initial disturbance of the reed might be reinforced by the acoustic feedback from the mouthpiece chamber as well as the resonator. Dalmont used an orifice as a non-linear acoustic absorber to thwart possible acoustic oscillations in the experimental measurement [9]. In this study, the open end of the resonator is replaced by an absorbing boundary condition (ABC) that is used as a pressure-reducing element and a nonlinear absorber that suppresses possible standing waves in the mouthpiece. On the other hand, the inside boundaries of the mouth cavity are also equipped with an ABC prescribed with non-zero pressure and velocity, functioning as both the flow source and an acoustic absorber.

The objectives of this paper are to obtain the complete non-linear characteristic curve including both the increasing and decreasing stage of mouth pressure to compare the flow behavior for cases corresponding to both fixed reed and moving reed and to verify the validity of the quasi-stationary model.

2. PREVIOUS WORK

The first result of experimentally measured characteristics of a single-reed instrument under steady flow conditions was given by Backus [1]. He fit his experimental results by a non-linear expression relating the volume flow U and the pressure difference Δp and the opening h , given as $U = 37\Delta p^{2/3}h^{4/3}$. However, Backus' empirical formula has not been verified by other researchers.

Assuming no pressure recovery from the reed channel to the air column input, most flow models describe the relationship between the volume flow and the pressure difference across the reed channel by means of the stationary Bernoulli equation ([2], [4], [3]), given as:

$$U = S_j \sqrt{\frac{2\Delta p}{\rho}}, \quad (1)$$

where ρ is the density of the air, $S_j = wh$ is the effective cross section of the jet, w is the effective width of the reed channel and h is the reed opening.

Then assuming the reed opening is linearly related to the pressure difference by its stiffness, the volume flow U can be described by the elementary model:

$$U = \begin{cases} wh \left(1 - \frac{\Delta p}{P_M}\right) \sqrt{\frac{2\Delta p}{\rho}}, & \text{if } \Delta p \leq P_M \\ 0, & \text{if } \Delta p > P_M \end{cases} \quad (2)$$

where P_M is the closing pressure of the reed channel. Since the Bernoulli equation is only valid for inviscid flow, the elementary model only holds for the case of relatively high Reynolds number ($Re = U/w\nu$), where w is the width of the reed used as the characteristic length, and ν is the kinematic viscosity of the fluid.

Hirschberg et al. [11] proposed a more complex flow model using numerical simulations which takes the effect of flow separation and friction into account. This model is improved and verified based on experimental results by Van Zon et al. ([12]). Depending on the geometry of the flow channel, which is characterized by L/h , where L and h are the length and the height of the flow channel respectively, there are two types of flows.

For short channels ($L/h \leq 1$), the flow is estimated by a contracted uniform flow

$$U = \alpha wh \sqrt{\frac{2\Delta p}{\rho}} \operatorname{sgn}(\Delta p), \quad (3)$$

where α is the dimensionless contraction parameter, typically found in the range of [0.5, 0.611] in Van Zon's measurement.

For long channels ($L/h \geq 4$), the flow is given by

$$U = \Omega \left[1 - \sqrt{1 - \frac{h^4(24c-1)\Delta p}{72\rho\nu^2(L-l_r)^2(1-\delta^*)^2}} \right] \quad (4)$$

$$\Omega = \frac{12\nu w(L-l_r)(1-\delta^*)^2}{h(24c-1)}$$

where ρ is the undisturbed density of the fluid, $\delta^* = 0.2688$ is a generalization of the boundary layer thickness for an arbitrary h , and $c = 0.0159$.

Dalmont et al. [9] measured the flow behavior using an artificial mouth-lip system and a real clarinet mouthpiece and found a flow behavior similar to that described by the quasi-stationary flow model. Interestingly, Almeida et al. [10] measured double-reed woodwind instruments and found that the normalized pressure flow characteristics of a bassoon and an oboe are similar to that of a clarinet and can be well described by the quasi-stationary model.

Da Silva [13] simulated the flow into a clarinet mouthpiece of different geometries using the lattice Boltzmann method for cases of both static and free oscillating reed. Da Silva's results agree well with Van Zon's model for both short and long reed channels in terms of vena contracta factor as a function of reduced Reynolds number as well as the volume flow as a function of pressure difference. However, the characteristic given in [13] is not complete because only a discrete number of values of mouth pressure were tested. Also, the simulation was less realistic because the flow was generated by a negative pressure source at the left end of the mouthpiece.

To obtain the complete curve of flow characteristics, the mouth pressure should continuously increase from zero to a maximum value until the reed reaches the lay such that the reed

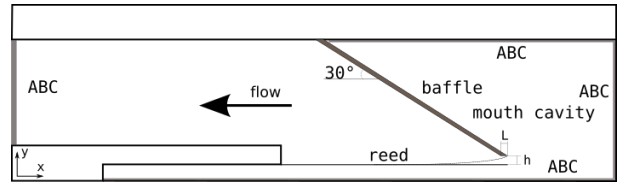


Figure 1: The LBM scheme of the mouthpiece and the mouth cavity.

channel is changing from fully opened to fully closed. Also, due to the viscoelasticity of the reed and the inertia and damping effects of the fluid, it is possible to observe a hysteresis effect due to the change of the rest position of the reed when closing versus when opening. This requires the measurement of the flow for both an increasing mouth pressure and a decreasing mouth pressure.

3. NUMERICAL PROCEDURE

In this study, we carried out the simulation of a mouthpiece-reed system of a clarinet using the two-dimensional LBM. On one hand, the relatively simple implementation of boundary conditions of the LBM allows us to easily explore different geometrical boundaries of a clarinet. On the other hand, the efficiency of our computation is greatly improved by using a parallel computing technique based on a low-cost Nvidia GPU graphic card installed on a personal computer. We used the multiple relaxation time (MRT) scheme [14] [15] and a relatively high numerical viscosity to maintain the numerical stability.

The LBM scheme, as depicted by Fig. 1, is described by thin walls resembling the cross section of a mouthpiece-reed system of a clarinet immersed in a fluid domain. The fluid domain is represented by a rectangular D2Q9 structure [16]. The domain boundaries along the solid walls of the mouthpiece are treated by a simple bounce-back scheme [17], which creates a no-slip condition at the wall and simulates a viscous boundary layer. The remaining boundaries have an absorbing boundary conditions prescribed with a zero velocity, as proposed by Kam et al. [18].

The size of the LB model representing the clarinet is given by $nX = 1240$ and $nY = 589$, which are the number of lattice cells along the x- and y-axes, respectively. The space resolution $dx = 8.5 \cdot 10^{-5} m$ representing the unit length of one lattice cell is determined by both the available computing resources and the smallest geometrical length of the boundary, which is the maximum value of the opening h of the reed channel. The number of lattice cells representing the height h is 14, which is sufficient in consideration of both stability and accuracy, according to our previous experiences. The time step is $dt = 1.44 \cdot 10^{-7} s$. To improve the numerical stability in the dynamic reed configuration, the lattice relaxation time is chosen as 0.532 and used in both static reed and dynamic reed cases, corresponding to a relatively high physical kinematic viscosity of $5.33 \cdot 10^{-4} m^2/s$.

The LB model is implemented by a custom parallel computing code written in Pycuda [19], and runs on a desktop PC equipped with a Nvidia GeForce GTX 670 graphics card. The speed-up factor is about 20 compared to the same model running on the CPU in serial mode.

The reed is based on the one-dimensional distributed model of a clamped-free bar with varying cross section and resolved with an implicit finite difference scheme, as proposed by Avanzini and Van Walstijn [20]. The length and width of the reed are specified as 34 mm and 13 mm, respectively. The

equilibrium tip opening is 1.2 mm. The external force component applied on the reed’s surface is calculated from the pressure field around the reed in each iteration, where the torsional and longitudinal modes are neglected. The interaction between the reed and the mouthpiece lay is considered to be inelastic, as discussed and justified in [20].

The problem of a moving curved boundary associated with the moving reed is solved by using an extrapolation scheme proposed by Guo et al [21]. This technique represents the no-slip condition and the transfer of momentum from the reed to the flow with an accuracy of second order. The displacement and the velocity of the reed is updated by the reed model based on the aerodynamic force upon the reed’s surface in each iteration, and the curved boundary is updated accordingly.

To eliminate the acoustic oscillation of the reed caused by the acoustic coupling of the chamber in the mouthpiece, an absorbing boundary scheme prescribed with a zero velocity, as proposed by Kam et al. [18], is placed along the cross-section at the left open end.

The source flow in the mouth is implemented using a variation of the absorbing boundary scheme, where the pressure of a non-zero target flow is prescribed with a customized profile. The pressure in the mouth cavity (pm) and in the mouthpiece chamber (pa), as well as the volume flow in the mouthpiece chamber (U) are measured, averaged and saved during the simulation. The pressure difference dp is calculated as $dp = pm - pa$. A typical duration of such a simulation is about 68 ms, or 500,000 iterations.

Two geometries of reed channel have been used in the simulation, namely the short channel ($L/h=1$) and the long channel ($L/h=4$), as depicted in Fig. 2.

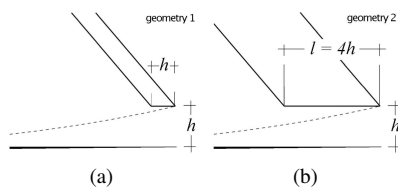


Figure 2: Two geometries of the reed channels: (a) short channel ($L/h=1$), (b) long channel ($L/h=4$).

Also, we conducted the simulation for both a static reed (stationary simulation) and a moving reed (dynamic simulation), respectively. There are two main differences between the present study and the previous work [13]. For the case of a static reed, the complete characteristic is measured continually for both increasing mouth pressure and decreasing mouth pressure. For the case of a moving reed, the disturbance of acoustic oscillations is minimized by using two approaches. One approach is to use a relatively slow change rate of the mouth pressure. Another approach is to use a higher fluid damping coefficient in Avanzini and Van Walstijn’s reed model, keeping key mechanical parameters such as Young’s modulus of elasticity and visco-elastic constant unchanged such that the mechanical characteristic of the reed is not affected.

4. RESULTS

4.1. Static Reed

The results of the stationary simulations for the cases of short channel and long channel (depicted in Fig. 2) are shown in Figs. 3 and 4, respectively.

Figures 3(a) and 4(a) depict the time history of the target pressure pmt prescribed on the absorbing boundary in the mouth cavity, the measured mouth pressure pm , the average pressure in the mouthpiece chamber pa and the pressure difference across the reed channel $dp = pm - pa$. In a typical simulation, the target pressure pmt increases linearly from zero to the highest value 9.5 kPa in a duration of about 28.87 ms (200,000 iterations, marked as Stage I) and holds for about 7.22 ms (50,000 iterations), then decreases linearly to zero in the duration of about 28.87 ms (marked as Stage II), and holds there for about 7.22 ms until the simulation is finished. The mouth pressure follows the pattern of pmt though at a reduced level. Since the reed is fixed, the reed channel is fully open during the course of the simulation and the mouth pressure never reaches the prescribed pressure due to the non-zero flow passing through the mouthpiece.

The measured flow U is compared to the Bernoulli flow Ub and the theoretical flow Uz calculated from Van Zon’s model for both short channel and long channel, as shown in Fig. 3(b) and 4(b), respectively. Since the opening and the width of the reed is fixed, the Bernoulli flow is only related to the measured pressure difference dp . Figures 3(c) and 4(c) represent the same flow data as a function of pressure difference, where $U(1)$ and $Uz(1)$ are the flows associated with Stage I, and $U(2)$, $Uz(2)$ are the flows associated with Stage II. The contraction parameter of Van Zon’s model for short channel is 0.7. In general, the measured flow is lower than the Bernoulli flow due to the flow separation occurring at the entrance of the reed channel. For the short channel, the measured flow is in good agreement with Van Zon’s model for most of the duration. However, for the long channel, the measured flow is significantly lower than the theoretical flow, which is only a little bit lower than the Bernoulli flow.

The phenomena of flow contraction, caused by the boundary layer effects on the walls of the lay and the reed and the flow separation at the entrance, can be quantitatively described by the vena contracta factors $vcf = U/Ub$, as depicted in Figs. 3(d) and 4(d), where $vcf(1)$ is associated to Stage I and $vcf(2)$ is associated to Stage II. The vena contracta factors of Van Zon’s model, noted as $vcf_z(1)$ and $vcf_z(2)$, corresponding to Stage I and Stage II respectively, are depicted in parallel.

In the case of the short channel, the measured vcf is in good agreement with theoretical vcf_z for most of the duration. In the case of the long channel, the measured vcf is significantly lower than the theoretical vcf_z . Also, the vcf corresponding to the long channel is lower than that of the short channel, which might be explained by the relatively higher damping in the long channel that is caused by friction from the flow and the walls.

A slight hysteresis effect can be observed in the region of low pressure difference for both geometries, i.e., $dp < 0.5$ for short channel and $dp < 1$ for long channel. Since the reed is fixed, the hysteresis phenomena cannot be caused by the viscoelasticity of the reed, rather, it is more likely due to the inertia of the air flow. We notice the variation of vcf is very small in about 80% of the duration of the simulation for both geometries, which suggests that a constant vcf used in the quasi-static model is a reasonable approximation for the case of a fixed reed.

4.2. Dynamic Reed

Throughout the dynamic simulations, the reed is moving as the pressure difference across the reed changes. The results corresponding to the short channel and the long channel are depicted in Figs. 5 and 6, respectively.

Figures 5(a) and 6(a) depict the time history of the tar-

get pressure p_{mt} prescribed on the absorbing boundary in the mouth cavity, the measured mouth pressure pm , the average pressure in the mouthpiece chamber pa and the pressure difference across the reed channel $dp = pm - pa$. The target pressure is prescribed in the same way as in the simulations of the fixed reed, i.e., p_{mt} increases linearly from zero to the highest value of 9.5 kPa, holds, and then decreases linearly and holds at zero until the simulation is finished.

Before the reed closes in Stage I, the mouth pressure increase along with p_{mt} , though at a reduced level. The pressure in the mouthpiece pa increases and reaches a peak value in about 9 (short channel) to 12 ms (long channel), then decreases because the amount of flow entering into the mouthpiece chamber is reduced due to a smaller opening of the reed channel. When the reed is completely closed at the closing pressure, which is about 8783 Pa for the short channel and 8939 Pa for the long channel, there is almost no flow entering into the mouthpiece chamber, and pa drops to zero. In Stage II, pa starts to increase when the decreasing mouth pressure is lower than the closing threshold. The threshold of the closing pressure in Stage II is lower than that in Stage I. This phenomenon is explained by the bifurcation delay, which is discussed in [22].

Figures 5(b) and 6(b) depict the reed channel opening as a function of dp for the case of short channel and long channel, respectively. For the most part, the opening is almost linearly related to dp . A hysteresis effect is found in the region of dp that is higher than about 7 kPa. There is a sudden drop and increase of opening when the mouth pressure reaches the closing pressure in Stage I and Stage II, respectively.

Figures 5(c) and 6(c) depict the Bernoulli flow Ub , the measured flow U and the theoretical flow Uz calculated from Van Zon's model as a function of time. Figures 5(c) and 6(c) represent the same flow data as a function of pressure difference, where $U(1)$, $Uz(1)$ and $U(2)$, $Uz(2)$ are the flow associated with Stage I and Stage II, respectively. The contraction parameter of Van Zon's model for short channel is 0.7.

The measured flow in the case of the moving reed shows some differences to the quasi-stationary model. The measured flow shows hysteresis for cases of both short channel and long channel. The quasi-stationary model, on the other hand, only shows hysteresis for the long channel because the displacement of reed is taken into account. For the short channel, the measured flow U is higher than the Bernoulli flow Ub and theoretical flow Uz of the quasi-stationary model in the region where dp is more than about 3 kPa. Similarly, for the long channel, U is higher than Ub and Uz in the region where dp is more than about 4 kPa. It can also be observed in Figures 5(e) and 6(e) that the vena contracta factor shows a value larger than unity in the region of higher dp . This phenomenon might be explained by the discussion in [9], where the quasi-stationary models assume the reed channel with a fixed separation point and a uniform height, which is questionable in the case of a more realistic clarinet mouthpiece. The discrepancies might also be related to the flows of low Reynolds number that cannot be described by the Bernoulli's equation. The measured vcf associated with the region of $dp > 6.5$ kPa is questionable and is discarded due to the dramatical change of both U and Ub , as depicted in the region around about 43 ms in Figures 5(c) and 6(c).

5. DISCUSSIONS AND CONCLUSIONS

The staircase-like ripples found in the measured flow and opening for the cases of moving reed (Figs. 5 and 6) might be studied from two aspects. The first influence comes from the mechanical oscillation of the reed initiated by the relatively quick

changing rate of the mouth pressure, especially in the decreasing stage of the pm curve. A slower changing rate can reduce the likelihood of acoustic oscillations at the cost of a prolonged simulation time. The measurements times reported in [9] are between 50 to 100 seconds, but this time scale is not practical in the current model even using parallel GPU computation. Another factor is related to the low spatial resolution. When the reed channel is nearly closed, the cells can be very few and insufficient to represent the flow crossing the reed channel and the boundary layer effect. This problem cannot be immediately solved by simply using an extremely large lattice because of the limited computation and memory resources allowed by the GPU device. An adaptive grid refinement technique [23] might be helpful but is not implemented in the current model yet. Nevertheless, a low-discretized lattice can still capture reasonable well global parameters such as the averaged volume flow.

Due to the relatively higher numerical viscosity, the Reynolds number in the numerical simulation is lower than the realistic one. In the situation of static reed, the highest Reynolds number is 140, which is much lower than the realistic Reynolds number 4762 (assuming the same volume velocity). Consequently, the measured flow is not exactly the same as the Bernoulli flow and the quasi-stationary model, which is based on the assumption of inviscid flow. A low numerical viscosity is not practical for the dynamic reed case because, apart from the issue of numerical stability, there is the difficulty of eliminating the noise caused by acoustic oscillations when the viscosity is very low. Nevertheless, useful results can still be obtained from the current model.

As already noted in Fig. 4(b), the predicted volume flow rate deviates largely from Van Zon's model for the long channel case. We attempted to investigate this discrepancy by estimating the boundary layer thickness from the spatial distribution and evolution of the jet. Figures 7(a) and 8(a) visualize the velocity field ($u = \sqrt{u_x^2 + u_y^2}$) for the cases of static short and long reed channels respectively, from which we can observe that the flow is passing through the reed channel and is dissipated in the mouthpiece chamber. Figures 7(b) and 8(b) depict the velocity profile of the jet passing through the short and long reed channel, respectively. In the short channel, a flow separation can be observed at the entrance and the total critical thickness of the boundary layers on both top and bottom walls is about 7 cells, corresponding to an averaged dimensionless thickness of 0.2333 for one wall, which is slightly lower than the thickness of 0.2688 used in Van Zon's model. For the case of long channel, a reattachment of the flow occurs after a distance on the order of the reed channel height, and a Poiseuille flow is developed after a transition zone. The averaged dimensionless thickness of the boundary layer is about 0.3 (9 cells in total). The lower volume flow for the long channel case might be caused by the boundary layer thickness which is slightly higher than that used in Van Zon's model. But it could also be influenced by the flow pattern characterized by a low Reynolds number, because the boundary layer thickness estimated from the velocity profile is not very accurate due to the low-discretization. In a dynamic situation, though, the flow profile would certainly not match Van Zon's assumption. The flow detachments at the reed tip can be better observed in Fig. 7(c) and 8(c), where the velocity profiles in the neighboring area of reed tip are depicted in a larger scale. The magnitude of the counter-flow at the reed wall is much lower than that of the maximum flow velocity but still can be observed.

The current LBM scheme is limited by its 2D nature, which is not fully capable of representing the 3D behavior of the real flow. Further, the flow measured from the mouthpiece-reed sys-

tem with a fully coupled acoustic resonator will be more realistic. This will be investigated in our next research project.

Acknowledgments

The authors wish to acknowledge funding from the Fonds québécois de la recherche sur la nature et les technologies (FQRNT), the Natural Sciences and Engineering Research Council of Canada (NSERC), and the Centre for Interdisciplinary Research in Music Media and Technology.

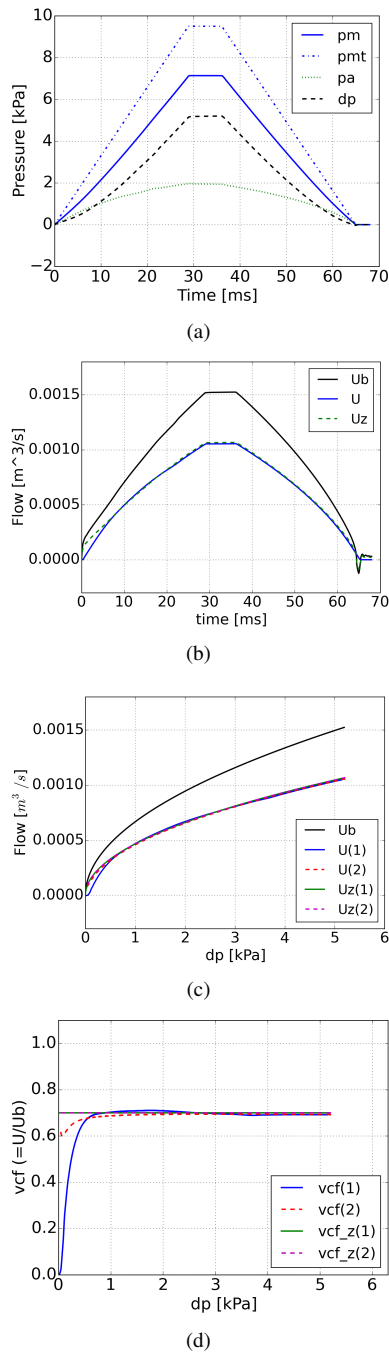


Figure 3: Static reed, short channel ($L/h = 1$): (a) pressure profile, (b) flow as function of time, (c) flow as function of pressure difference, and (d) vcf as function of pressure difference.

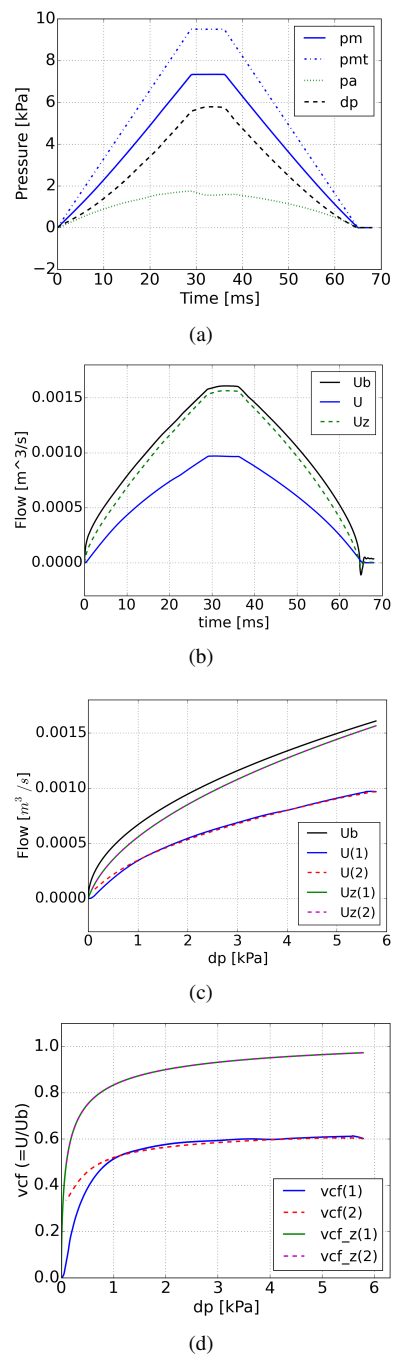
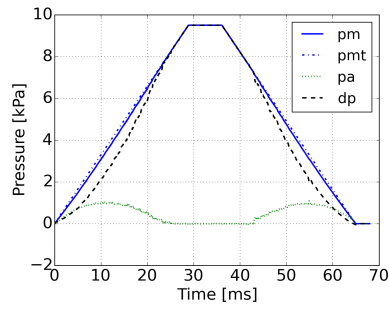
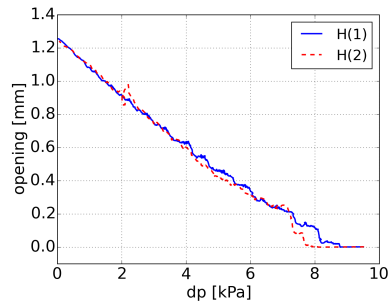


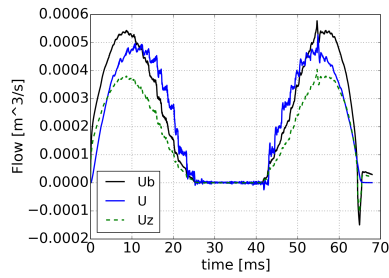
Figure 4: Static reed, long channel ($L/h = 4$): (a) pressure profile, (b) flow as function of time, (c) flow as function of pressure difference, and (d) vcf as function of pressure difference.



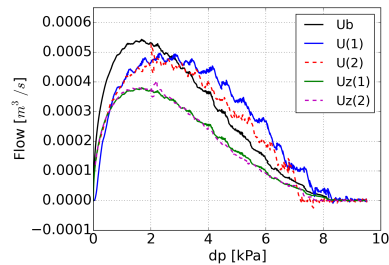
(a)



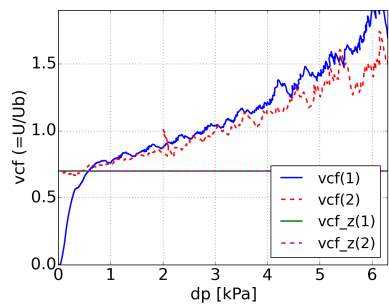
(b)



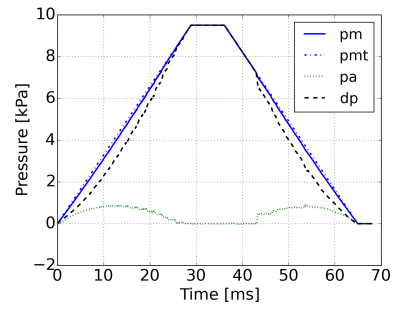
(c)



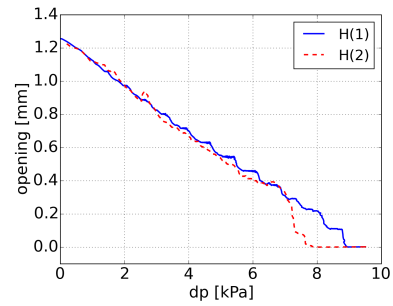
(d)



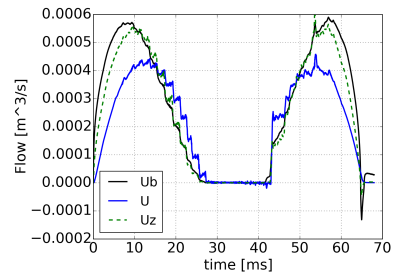
(e)



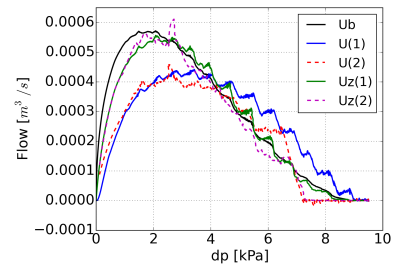
(a)



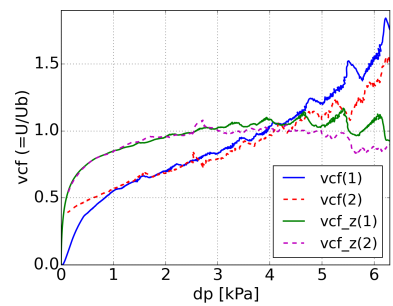
(b)



(c)



(d)



(e)

Figure 5: Moving reed, short channel ($L/h = 1$): (a) pressure profile, (b) opening as function of pressure difference, (c) flow as function of time, (d) flow as function of pressure difference, and (e) vcf.

Figure 6: Moving reed, long channel ($L/h = 4$): (a) pressure profile, (b) opening as function of pressure difference, (c) flow as function of time, (d) flow as function of pressure difference, and (e) vcf.

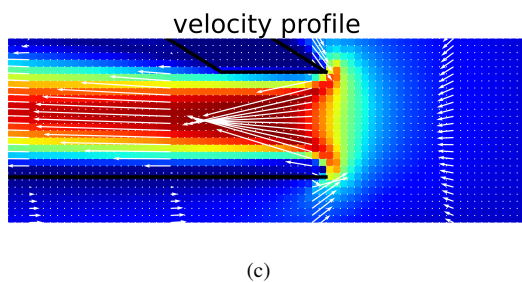
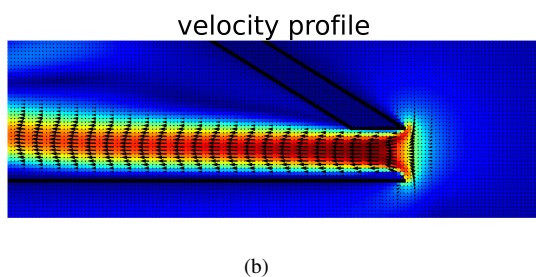
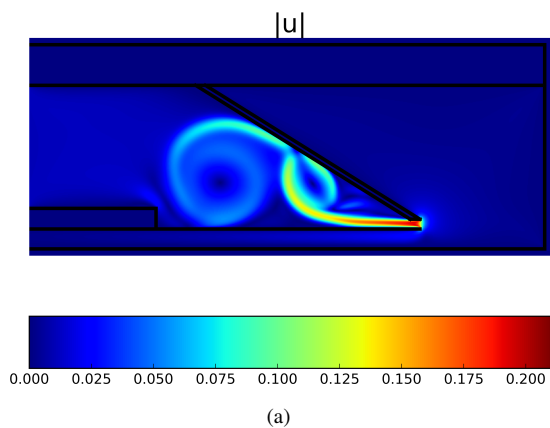


Figure 7: Velocity field, static short reed channel: (a) absolute velocity, (b) velocity profile of the jet passing through the reed channel, (c) velocity profile depicted in a larger scale.

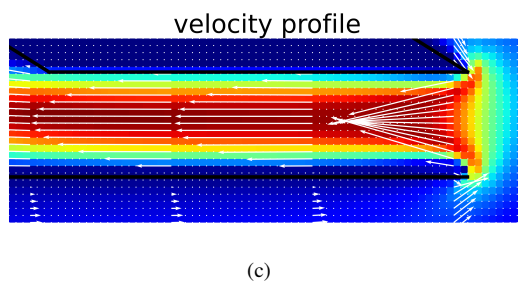
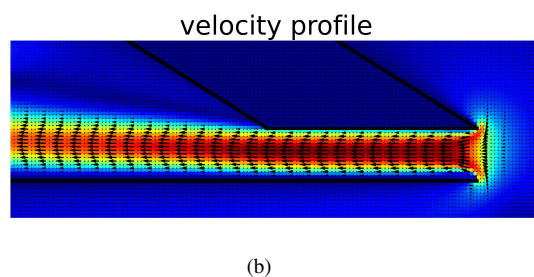
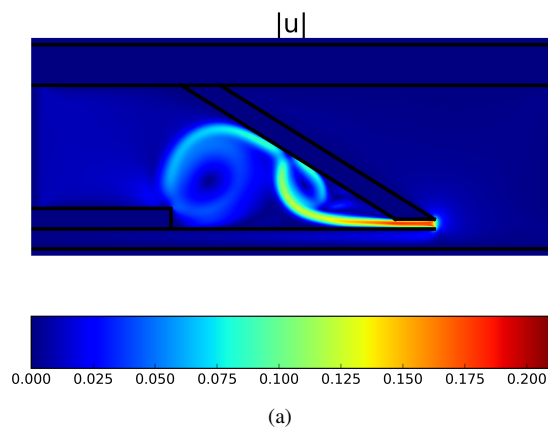


Figure 8: Velocity field, static long reed channel: (a) absolute velocity, (b) velocity profile of the jet passing through the reed channel, (c) velocity profile depicted in a larger scale.

6. REFERENCES

- [1] John Backus, “Small-vibration theory of the clarinet,” *The Journal of the Acoustical Society of America*, vol. 35, no. 3, pp. 305–313, 1963.
- [2] Theodore A Wilson and Gordon S Beavers, “Operating modes of the clarinet,” *The Journal of the Acoustical Society of America*, vol. 56, no. 2, pp. 653–658, 1974.
- [3] Junich Saneyoshi, H Teramura, and S Yoshikawa, “Feedback oscillations in reed woodwind and brasswind instruments,” *Acta Acustica united with Acustica*, vol. 62, no. 3, pp. 194–210, 1987.
- [4] Neville H Fletcher, “Autonomous vibration of simple pressure-controlled valves in gas flows,” *The Journal of the Acoustical Society of America*, vol. 93, no. 4, pp. 2172–2180, 1993.
- [5] Jean Kergomard, “Elementary considerations on reed-instrument oscillations,” *Courses and lectures-international centre for mechanical sciences*, pp. 229–290, 1995.
- [6] Jean Kergomard, Sébastien Ollivier, and Joel Gilbert, “Calculation of the spectrum of self-sustained oscillators using a variable truncation method: Application to cylindrical reed instruments,” *Acta Acustica united with Acustica*, vol. 86, no. 4, pp. 685–703, 2000.
- [7] S Ollivier, J-P Dalmont, and J Kergomard, “Idealized models of reed woodwinds. part i: Analogy with the bowed string,” *Acta acustica united with acustica*, vol. 90, no. 6, pp. 1192–1203, 2004.
- [8] S Ollivier, Jean Kergomard, and Jean-Pierre Dalmont, “Idealized models of reed woodwinds. part ii: On the stability of,” *Acta acustica united with acustica*, vol. 91, no. 1, pp. 166–179, 2005.
- [9] Jean-Pierre Dalmont, Joël Gilbert, and Sébastien Ollivier, “Nonlinear characteristics of single-reed instruments: Quasistatic volume flow and reed opening measurements,” *The Journal of the Acoustical Society of America*, vol. 114, no. 4, pp. 2253–2262, 2003.
- [10] André Almeida, Christophe Vergez, and René Caussé, “Quasistatic nonlinear characteristics of double-reed instruments,” *The Journal of the Acoustical Society of America*, vol. 121, no. 1, pp. 536–546, 2007.
- [11] A. Hirschberg, R. W. A. van de Laar, J. P. Marrou-Mauriere, A. P. J. Wijnands, H. J. Dane, S. G. Kruijswijk, and A. J. M Houtsma, “A quasi-stationary model of air flow in the reed channel of single-reed wind instruments,” *Acustica*, vol. 70, 1990.
- [12] J. Van Zon, A. Hirschberg, J. Gilbert, and A. P. J. Wijnands, “Flow through the reed channel of a single reed instrument,” in *J. Phys., Paris, Colloq. 54, C2 821824*, 1990.
- [13] A. R. da Silva, *Numerical Studies of Aeroacoustic Aspects of Wind Instruments*, Ph.D. thesis, McGill University, Montreal, Canada, 2008.
- [14] Dominique d’Humières, “Generalized lattice-boltzmann equations,” *Rarefied gas dynamics- Theory and simulations*, pp. 450–458, 1994.
- [15] Zhaoli Guo and Chang Shu, *Lattice Boltzmann Method and Its Applications in Engineering*, World Scientific Publishing, 2013.
- [16] Y.H. Qian, D. d’Humières, and P. Lallemand, “Lattice BGK models for Navier-Stokes equation,” *Europhysics Letters*, vol. 17, no. 6, pp. 479–484, 1992.
- [17] S. Succi, *The lattice Boltzmann equation for fluid dynamics and beyond*, Oxford University Press, 2001.
- [18] E.W.S. Kam, R.M.C. So, and R.C.K. Leung, “Non-reflecting boundary conditions for one-step LBM simulation of aeroacoustics,” in *27th AIAA Aeroacoustics Conference, 8-10 May 2006, Cambridge, Massachusetts*, 2006.
- [19] Andreas Klöckner, Nicolas Pinto, Yunsup Lee, Bryan Catanzaro, Paul Ivanov, Ahmed Fasih, AD Sarma, D Nanongkai, G Pandurangan, P Tetali, et al., “Pycuda: Gpu run-time code generation for high-performance computing,” *Arxiv preprint arXiv*, vol. 911, 2009.
- [20] Federico Avanzini and Maarten van Walstijn, “Modelling the mechanical response of the reed-mouthpiece-lip system of a clarinet. part i. a one-dimensional distributed model,” *Acta Acustica united with Acustica*, vol. 90, no. 3, pp. 537–547, 2004.
- [21] Zhaoli Guo, Chuguang Zheng, and Baochang Shi, “An extrapolation method for boundary conditions in lattice boltzmann method,” *Physics of Fluids (1994-present)*, vol. 14, no. 6, pp. 2007–2010, 2002.
- [22] Baptiste Bergeot, André Almeida, Bruno Gazengel, Christophe Vergez, and Didier Ferrand, “Response of an artificially blown clarinet to different blowing pressure profiles,” *The Journal of the Acoustical Society of America*, vol. 135, no. 1, pp. 479–490, 2014.
- [23] M. Rohde, D. Kandhai, J. J. Derksen, and H. E. A. van den Akker, “A generic, mass conservative local grid refinement technique for lattice-boltzmann schemes,” *International Journal for Numerical Methods in Fluids*, vol. 51, no. 4, pp. 439–468, 2006.